

Orientation and Microenvironment of Naphthalene Guest in the Host Nanoporous Phase of Syndiotactic Polystyrene

Vincenzo Venditto,[†] Giuseppe Milano,[‡] Anna De Girolamo Del Mauro,[§] and Gaetano Guerra^{*,||}

Dipartimento di Chimica, Università di Salerno, 84081 Baronissi (Salerno), Italy

Jun Mochizuki and Hideyuki Itagaki^{*,⊥}

Department of Chemistry, Graduate School of Electronic Science and Technology and School of Education, Shizuoka University, 836 Ohya, Shizuoka 422-8529, Japan

Received October 15, 2004; Revised Manuscript Received February 18, 2005

ABSTRACT: Syndiotactic polystyrene (s-PS) films including a fluorescent guest (naphthalene, NP) in their nanoporous δ crystalline phase have been prepared and characterized by X-ray diffraction, infrared linear dichroism, molecular modeling, and fluorescence depolarization techniques. A nearly perpendicular orientation of the fused rings of NP guest molecules with respect to the chain axis of the δ crystalline structure has been established by molecular mechanics and by evaluation of directions of transition moment vectors of infrared vibrational modes. The fluorescence depolarization is more efficient for NP guest molecules into the host phase than for NP molecules simply absorbed in the amorphous phase. This could be due to a more efficient resonance energy transfer between guest molecules, possibly associated with their ordered positioning and orientation into the host nanoporous polymeric crystallites.

1. Introduction

Recent studies relative to the polymorphic behavior of syndiotactic polystyrene (s-PS) have shown that one of its four crystalline forms (the δ form) is nanoporous and has a density (0.977 g/cm³) definitely lower than amorphous s-PS (1.04 g/cm³), which is close to that one of atactic polystyrene.¹

The monoclinic structure of δ form of s-PS (space group $P2_1/a$; $a = 1.74$ nm; $b = 1.18$ nm; $c = 0.77$ nm; $\gamma = 117^\circ$) has per unit cell two identical cavities centered on the center of symmetry and bounded by 10 phenyl rings (Figure 1A,A').^{1,2} By sorption of generally isolated guest molecules into these cavities, as well as by different solution crystallization procedures, clathrate phases^{1–4} are easily achieved. In particular, the crystalline cavities of the nanoporous δ phase are large enough to absorb as guest, without any substantial distortion of the host lattice, isolated molecules as large as 1,2-dichloroethane.^{2,4} Moreover, associated with small distortions of the lattice (essentially increases of the b axis up to 10–15%) bigger guests, as toluene can be hosted.^{2,3a} Suitable procedures for guest removal, generally involving its replacement by more volatile temporary guests (like acetone, CS₂ or CO₂), allow to easily regenerate the nanoporous form.⁵

Sorption studies from liquid and gas phases, have shown that δ -form s-PS samples are able to absorb suitable guest molecules, even when present at very low concentrations.^{6–9} In particular, it has been clearly demonstrated that for sorption at low activities, or after partial desorption, some penetrants can be located essentially only as guest into the crystalline phase, while their concentration in the amorphous phase can be negligible.^{6b,7}

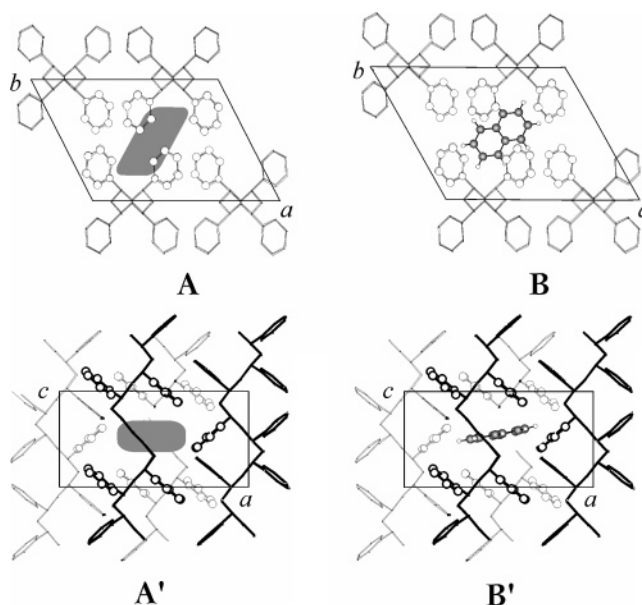


Figure 1. Models of packing and unit cell for crystal structures of s-PS: (A) nanoporous δ form; (B) s-PS/NP clathrate phase, presenting the calculated minimum energy location of naphthalene. In particular, the unit cells are shown for two different views, along c (A, B) and perpendicular to the ac plane (A', B'). The 10 phenyl rings which confine the cavity or the NP guest are represented by stick and balls. The region of empty space calculated for the δ phase² is dotted in A and A'.

The achievement of s-PS films, being also of high thickness, which present high degrees of axial^{1,4,10} or planar^{11,12} crystalline phase orientations has been also described. In particular, for uniaxially stretched films, by combined infrared linear dichroism and X-ray diffraction measurements and molecular modeling, information relative to the orientation and mobility of different chlorinated guests of the nanoporous δ phase has been recently achieved.¹⁰

[†] E-mail: vvenditto@unisa.it.

[‡] E-mail: gmilano@unisa.it.

[§] E-mail: adelmauro@unisa.it.

^{||} E-mail: gguerra@unisa.it.

[⊥] E-mail: edhitag@ipc.shizuoka.ac.jp.

In this paper analogous infrared dichroism and X-ray diffraction analyses have been effected for naphthalene (NP), which is a fluorescent guest molecule. The guest fluorescence gives the opportunity to get additional information on the guest microenvironment by using the fluorescence depolarization technique. In fact, fluorescence depolarization is an effective tool to characterize mobility of guest small molecules as well as dynamic local motions of macromolecules, though it does not appear to be applied to polymer characterization so extensively.^{13–15} As an example of previous application of fluorescence depolarization method, some of the authors doped isotactic polystyrene- (iPS-) decalin gels with several fluorescent molecules of different molecular sizes and measured their fluorescence depolarization to monitor the mobility of the fluorescent molecules.¹⁶

In this paper, in the attempt to get additional information on host-guest interactions in the nanoporous δ phase of sPS, the fluorescence depolarization behaviors in s-PS films of NP molecules, being a guest of the nanoporous δ phase or simply absorbed in the amorphous phase, have been compared.

2. Experimental Section

2.1. Materials. Naphthalene was purchased from Carlo Erba and used without further purification.

Syndiotactic polystyrene was supplied by Dow Chemical under the trademark Qwestra 101. ¹³C nuclear magnetic resonance characterization showed that the content of syndiotactic polystyrene triads was over 98%. The weight-average molar mass obtained by gel permeation chromatography (GPC) in trichlorobenzene at 135 °C was found to be $M_w = 3.2 \times 10^5$ with the polydispersity index being $M_w/M_n = 3.9$.

Unoriented s-PS amorphous films have been obtained by extrusion of the melt with an extrusion head of 200 mm \times 0.5 mm. Unoriented s-PS amorphous films including naphthalene have been obtained by exposure for 5 days to NP vapors at room temperature.

Oriented films, 20–30 μ m thick, have been obtained by monoaxial stretching of the extruded ones, at different draw ratios up to $\lambda \approx 3$, at a constant deformation rate of 0.1 s⁻¹, in the temperature range 105–110 °C with a Bruker stretching machine.

Unoriented and axially oriented s-PS/NP clathrate films have been obtained from unoriented and oriented films, by exposure to NP vapors at 60 °C.

Axially oriented α form films have been obtained by annealing at 200 °C of stretched s-PS/NP clathrate films. The NP sorption, in the α form films, was achieved by exposure to NP vapors at 60 °C.

All samples, after NP treatments, have been maintained in air at least for 7 days before measurements. The content of naphthalene molecules, as determined by thermogravimetric analysis (TGA), in the films which have been used for the fluorescence measurements, is in the range 0.5–1 wt % for amorphous and α form films while in the range 1–2.5 wt % for δ form films.

2.2. X-ray Diffraction. Wide-angle X-ray diffraction patterns with nickel filtered Cu K α radiation were obtained, in reflection, with an automatic Bruker D8 Advance diffractometer.

For the uniaxially stretched films, the *degree of axial orientation* ($f_{c, \text{RX}}$), that is of the orientation of the chain axes of the crystalline phase with respect to the stretching direction, has been formalized on a quantitative numerical basis using the usual Hermans orientation function¹⁷

$$f_{c, \text{RX}} = \frac{\overline{\cos^2 \gamma} - 1/2}{1/2} \quad (1)$$

where $\overline{\cos^2 \gamma}$ is the squared average cosine value of the angle,

γ , between the crystallographic c (chain) axes and the stretching direction.

The quantity $\overline{\cos^2 \gamma}$ has been experimentally evaluated, for both NP clathrate and α form films, by

$$\overline{\cos^2 \chi_{002}} = \frac{\int_0^{\pi/2} I(\chi_{002}) \cos^2 \chi_{002} \sin \chi_{002} d\chi_{002}}{\int_0^{\pi/2} I(\chi_{002}) \sin \chi_{002} d\chi_{002}} \quad (2)$$

where $I(\chi_{002})$ is the intensity distribution of the (002) diffractions on the Debye rings and χ_{002} is the azimuthal angle measured from the meridian. The diffracted intensities $I(\chi_{002})$ were obtained by using an AFC7S Rigaku automatic diffractometer, and were collected sending the X-ray beam perpendicular to the film surface. Because the collection was performed at constant 2θ values and in the equatorial geometry, the Lorentz and polarization corrections were unnecessary.

In these assumptions, when $f_{c, \text{RX}}$ is equal to 1, the c axes of all crystallites are perfectly parallel to the stretching direction. The orientation factor is equal to zero for random orientation.

2.3. Infrared Spectroscopy. Infrared spectra were obtained at a resolution of 2.0 cm⁻¹ with a Vector 22 Bruker spectrometer equipped with deuterated triglycine sulfate (DTGS) detector and a KBr beam splitter. The frequency scale was internally calibrated to 0.01 cm⁻¹ using a He-Ne laser. 32 scans were signal averaged to reduce the noise. Polarized infrared spectra were recorded by the use of a SPECAC 12500 polarizer.

As far as infrared spectroscopy is concerned, the axial orientation function is given by¹⁸

$$f_{c, \text{IR}} = \frac{(R - 1)(2 \cot^2 \alpha + 2)}{(R + 2)(2 \cot^2 \alpha - 1)} \quad (3)$$

where $R = A_{\parallel}/A_{\perp}$ is the dichroic ratio, A_{\parallel} and A_{\perp} being the measured absorbance for electric vectors parallel and perpendicular to the draw direction respectively, and α being the angle between the chain axis and the transition moment vector of the vibrational mode.

For the evaluation of the α angle relative to transition moment vectors of the NP vibrational modes, the orientation factor relative to the helical chains of the host polymer phase ($f_{c, \text{IR}}$) has been evaluated by the dichroic ratio of the 571 cm⁻¹ infrared band.¹⁰

As usual, an order parameter S can be defined as the ratio:

$$S = (R - 1)/(R + 2) \quad (4)$$

As for the dichroism measurements, only samples presenting an NP content lower than 2% have been used. This ensures that for the δ form films the NP molecules are only present as guest of the nanoporous phase.

2.4. Fluorescence Depolarization Technique. Fluorescence spectra, fluorescence excitation spectra, and fluorescence depolarization were measured at 25 °C on a Hitachi F-4500 spectrofluorometer. Fluorescence measurements for the s-PS films including NP molecules were carried out by placing the films between two quartz disks. Films were set at 45° to the exciting beam whose shape on a film is rectangular with 1.3 cm long and 1 mm high. To determine the values of NP fluorescence anisotropy a Hitachi automatic polarizer was attached to a Hitachi F-4500 spectrofluorometer: the anisotropic values were determined by measuring values for 100 sec at some wavelengths more than three times and averaging them. Excitation wavelength was 280 nm and emission wavelengths were 326, 337, and 350 nm.

To determine the intrinsic anisotropy values of NP molecules whose motions are completely suppressed, we measured the fluorescence anisotropy of atactic polystyrene (a-PS) films doped with some different concentrations of NP. The films were prepared on quartz disks by using a spin-casting method from a 1% THF solution of a-PS (Tosoh Corp.; $M_w = 9.64 \times 10^4$, $M_w/M_n = 1.01$), with different amounts of NP, and dried by

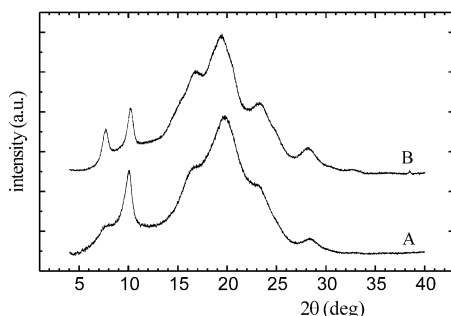


Figure 2. X-ray diffraction patterns collected by an automatic diffractometer (Cu K α radiation) of s-PS samples presenting the s-PS/NP clathrate phase with a NP content close to 5 wt %: (A) film; (B) powder.

extensive pumping under vacuum for more than 3 days at 40 °C. More than four films were prepared to ascertain the reproducibility. The films were left on the quartz disks for ease of handling during subsequent measurements and were set at 45° to the exciting beam for the measurements.

In general, when a chromophore is excited by polarized light, the emission of the chromophore will be observed to be polarized if (I) the molecular motion of the chromophore is slow enough and (II) energy transfer and/or energy migration does not take place. Therefore, measurement of the emission anisotropy yields information about the molecular motions and/or energy transportation. The fluorescence anisotropy, r , is defined as

$$r = (I_p - G I_v) / (I_p + 2 G I_v) \quad (5)$$

where I_p and I_v denote the measured intensities when the observing polarizer is parallel and perpendicular, respectively, to the direction of the polarized excitation, and G is a machine constant. When the motion of a chromophore is fast enough or if the excitation energy can hop among molecules, the anisotropy of the emission falls to zero.

2.5. Computational Methods. Vibrational frequencies calculations have been performed by density functional theory (DFT) method after geometry optimization at B3LYP/6-31G** level. The transition moment direction for the i -normal mode has been obtained from electric dipole moment (μ) derivatives $\partial\mu/\partial Q_i$ (indicated as $\mu_i^{(i)}$ in Figure 4) with respect to the corresponding i -normal coordinate (Q_i).¹⁹ Details about molecular mechanics procedures for the considered host–guest systems and force field are reported in ref 7d. All calculations have been performed by the Gaussian98 program.²⁰

3. Results and Discussion

3.1. X-ray Diffraction Characterization. The X-ray diffraction pattern of an amorphous s-PS extruded film after absorption of NP vapor at 60 °C for 3 h (followed by NP desorption at 50 °C for 6 days) and presenting a NP content close to 5 wt % is shown in Figure 2A. This pattern presents diffraction peaks at $2\theta \approx 7.7, 10.2, 16.9, 19.5, 23.3$, and 28.3° for Cu K α radiation, corresponding to 010, 210, 111, $\bar{3}21/301$, $\bar{4}11/\bar{4}21$, and 302/322, respectively, typical of s-PS clathrate phases,^{1,3,4} and hence clearly indicates the NP induced formation of a s-PS/NP clathrate phase. A comparison with the diffraction pattern of a s-PS/NP clathrate powder (Figure 2B) indicates that the relative intensities of the diffraction peaks are poorly altered, thus showing that the NP induced crystallization on extruded films, contrary to other guest induced crystallizations,^{16b} leads to substantially unoriented clathrate films.

As for the uniaxially stretched films, the achievement of NP clathrate and α phases have been confirmed by X-ray diffraction photographic patterns (not shown).

Both crystalline phases present a simple *axial orientation*; that is, the c axis (corresponding as usual to the chain axis) is preferentially oriented parallel to the stretching direction. This is pointed out by the similarity of the X-ray diffraction photographic patterns taken with X-ray beam perpendicular or parallel to the film surface.

X-ray diffraction data of the uniaxially stretched clathrate films can be used to obtain accurate information relative to the crystalline structure of the polymeric host. However, the information, which can be achieved by X-ray diffraction analysis, relative to the guest orientation within the host cavity is much less accurate.^{3,4} In fact, the usual procedure comprises a molecular mechanics evaluation of the guest orientation which is subsequently validated and refined by quantitative comparison between experimental and calculated diffraction intensities. However, the accuracy in this evaluation of guest orientation is low due to the generally poor dependence of the calculated diffraction intensity on the guest orientation, to the lack of direct information on the fraction of filled crystalline cavities as well as to the guest mobility being much higher than the host mobility.

For this reason, in the present paper, we have preferred to get information on the orientation of the guest molecules into the host cavity by the infrared dichroism method recently described by some of us, for some s-PS chlorinated guests.¹⁰ It is worth noting that this procedure gives a direct evaluation of the angle of the transition moment vector of several guest vibrational modes with respect to the chain polymer axis. Moreover, this infrared method gives the opportunity to find film preparation conditions for which guest molecules are located essentially only into the crystalline phase,¹⁰ and it also presents the advantage that the results are independent of the degree of filling of the crystalline cavities of the nanoporous phase.

3.2. Infrared Dichroism Analysis. FTIR spectra of the uniaxially stretched (at $\lambda \approx 3$) semicrystalline s-PS films including NP molecules, for the wavenumber range 1400–450 cm^{-1} and taken with polarization plane parallel and perpendicular to the draw direction, are shown in Figure 3. The spectra of Figure 3, parts A and B, refer to films presenting the NP clathrate and the α phase, respectively, and both present several dichroic peaks.

In particular, the spectrum of the semicrystalline sample including the NP clathrate phase (Figure 3A) presents highly dichroic helical peaks of the polymer host (labeled by **h**) at 501(\perp), 548(\perp), 571(\parallel), 769(\parallel), 933(\perp), 944(\parallel), 969(\perp), 978(\perp), 1039(\parallel), 1277(\parallel), 1320(\perp), 1353(\parallel) cm^{-1} ,^{10,21,22} as well as dichroic peaks of the NP guest (labeled by **N**) at 478(\parallel), 618(\perp), 786(\parallel), 845(\perp), 960(\parallel), 1009(\perp), 1128(\perp), 1211(\perp), 1243(\perp), 1268(\perp), 1389(\perp) cm^{-1} .^{23–25} On the other hand, the spectrum of the α phase semicrystalline film (Figure 3B) shows highly dichroic trans-planar polymer peaks (labeled by **t**) at 540(\parallel), 902(\parallel), 1222(\parallel), 1334(\perp), 1350(\parallel) and 1374(\perp) cm^{-1} ,^{26,27} and a nearly negligible dichroism of the NP peaks (labeled by **N**).

These observations can be easily rationalized by considering that NP molecules are only absorbed in the essentially unoriented amorphous phase of the stretched α form films, while they are mostly enclosed as guest of the highly oriented clathrate phase into the stretched clathrate films. The dichroism of the NP peaks, for the

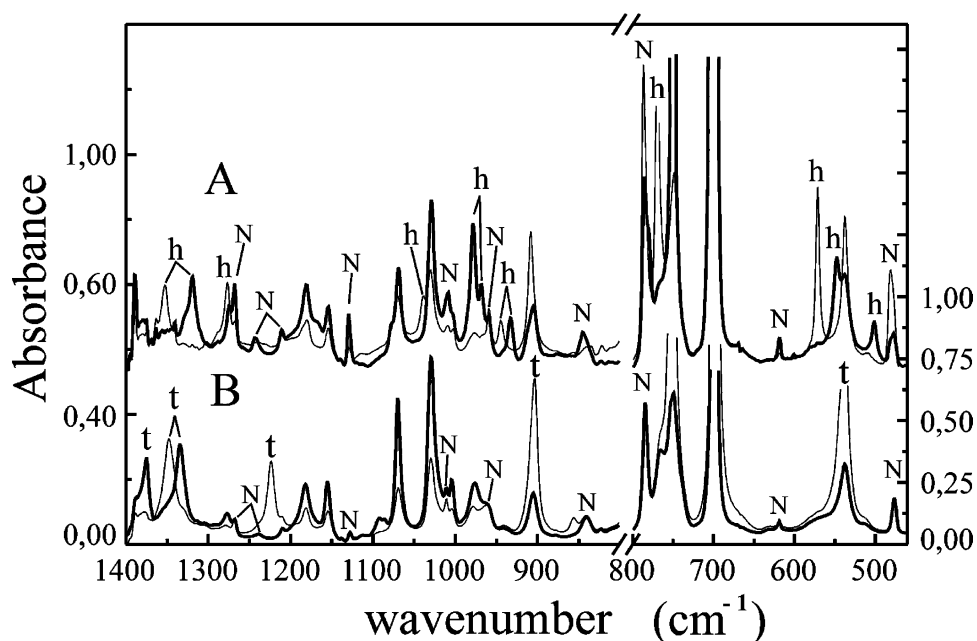


Figure 3. FTIR spectra for the wavenumber range 1400–450 cm^{-1} , taken with polarization plane parallel (thin lines) and perpendicular (thick lines) to the draw direction, for uniaxially stretched s-PS films (for $\lambda \approx 3$) including the following: (A) 8 wt % of NP in the δ crystalline phase; (B) 4 wt % of NP in the amorphous phase and a guest-free crystalline α phase. The labels **h**, **t**, and **N** refer to absorbance peaks of helical polymer chains of the host δ phase, of trans-planar polymer chains of the α crystalline phase and of NP, respectively.

Table 1. Infrared Absorbance Peaks of Naphthalene for Which the Vibrational and Dichroism Analyses Have Been Effectuated^a

| sym | mode | calcd (cm^{-1}) | exp. (cm^{-1}) | α (deg) | α_{calc} (deg) |
|----------|------------|----------------------------|---------------------------|----------------|------------------------------|
| B_{3u} | ν_6 | 492 | 478 | 30 ± 1 | 16 |
| | ν_{20} | 981 | 960 | 41 ± 1 | |
| B_{2u} | ν_{23} | 1039 | 1009 | 64 ± 1 | 72 |
| | ν_{29} | 1233 | 1211 | 58 ± 1 | |
| B_{1u} | ν_{25} | 1144 | 1128 | 67 ± 1 | 82 |
| | ν_{33} | 1408 | 1389 | 60 ± 1 | |

^a For each vibrational mode, α and α_{calc} are the angles between the transition moment vectors and the c axis of the host crystalline phase, as experimentally evaluated by dichroism measurements and as evaluated by molecular modeling, respectively.

clathrate film, clearly indicates the presence of some preferential orientation of the guest molecules with respect to the stretching direction.

As discussed in detail in ref 10, since the transition moment vector for the helical host band at 571 cm^{-1} is parallel to the chain axis, the order parameters for this host helical band can be directly used as a measure of the axial orientation factor of the crystalline phase ($f_{c,\text{IR}}$). In particular, for the uniaxially stretched films presenting the NP clathrate phase of Figure 3A, $f_{c,\text{IR}}$ is close to 0.96 and well compares with the value of the orientation of the crystalline phase as obtained by X-ray diffraction measurements (section 2.2).

3.3. NP Guest Orientation with Respect to the Chain Axis of the Host Crystalline Phase. Direct information relative to the orientation of the guest with respect to the chain axis of the polymeric crystalline host can be easily achieved by infrared dichroism measurements on films uniaxially stretched at different draw ratios, as recently reported for some chlorinated guests of s-PS clathrate phases in ref.10.

Particularly informative are the infrared NP peaks listed in Table 1, well resolved in the spectra of Figure 3 and attributed to B_{1u} , B_{2u} , or B_{3u} normal modes.^{23–25}

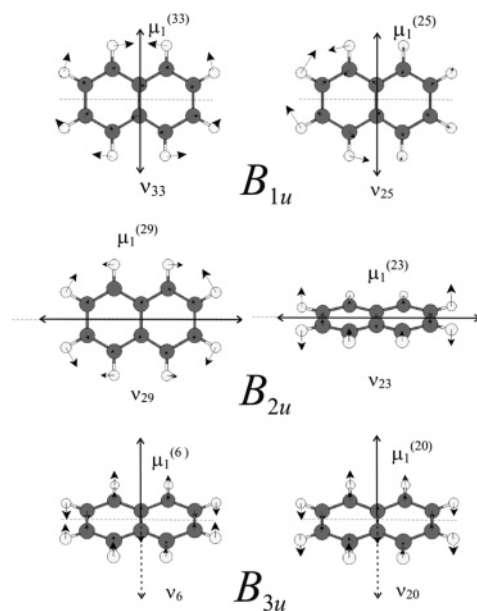


Figure 4. Vibrational modes and transition moment vector directions $\mu_1^{(i)}$, as calculated for the NP infrared peaks of Table 1.

These vibrational modes as well as the calculated transition moment vector directions $\mu_1^{(i)}$ are shown in Figure 4.

By using a procedure analogous to that one described in ref 10, a quantitative comparison between dichroic ratios of a polymer host helical peak and of the guest peaks of Table 1 is presented in Figure 5. In particular, the infrared order parameter S , as evaluated by dichroic ratios of the NP guest peaks are reported vs the orientation factors relative to the helical chains of the clathrate phases, as evaluated by the dichroic ratio of the 571 cm^{-1} infrared peak ($f_{c,\text{IR}}$). By applying eq 3 to the data of Figure 5, α values in the ranges 30°–41° and 58°–67° have been obtained, for all the considered

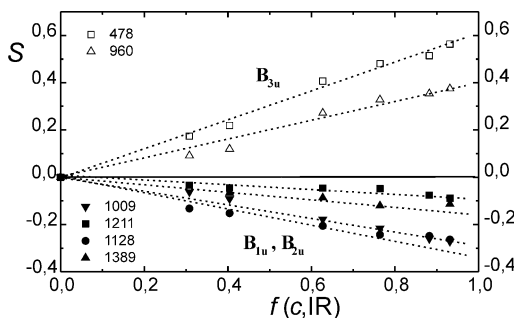


Figure 5. Infrared order parameter S , as evaluated by dichroic ratios of the NP peaks of Table 1, for NP guest molecules, vs the orientation factor of the helical chains of the host polymer phase ($f_{c,IR}$). Empty and filled symbols refer to peaks corresponding to NP out-of-plane (B_{3u} modes) and in-plane (B_{2u} and B_{1u} modes) vibrational modes, respectively. The wavenumber of the peaks, as cm^{-1} , are reported close to the symbols.

NP out-of-plane (B_{3u} symmetry) and in-plane (B_{2u} and B_{1u} symmetries) vibrational modes, respectively (fifth column of Table 1).

A molecular modeling analysis, analogous to that one described in refs 7d and 10, shows that the energy minimum location of naphthalene into the crystalline cavity (Figure 1B) presents the fused rings plane roughly perpendicular to the chain axis. In particular, the angle between the chain axis and the mutually orthogonal transition moment vectors of B_{1u} , B_{2u} or B_{3u} modes are 82, 72, and 16°, respectively (α_{calc} , sixth column of Table 1).

A comparison between the data of the two last columns of Table 1 shows that, for all the considered (both in plane and out of plane) peaks, the experimental α value, obtained by the FTIR dichroism data, are always located between the corresponding calculated value and the magic angle (54.7°). Hence, the obtained results confirm a roughly perpendicular orientation of the NP fused rings with respect to the chain axis of the crystalline phase and suggest the presence of some limited mobility with respect to the average minimum energy position, as already observed for some chlorinated guest molecules.¹⁰

A validation of the experimental α values which have been obtained by the procedure described in Figure 4 is given by evaluation of

$$\cos^2 \alpha_{B_{1u}} + \cos^2 \alpha_{B_{2u}} + \cos^2 \alpha_{B_{3u}} \quad (6)$$

where $\alpha_{B_{1u}}$, $\alpha_{B_{2u}}$, and $\alpha_{B_{3u}}$ are the average of the α values (listed in the fifth column of Table 1) obtained for the NP B_{1u} , B_{2u} , or B_{3u} modes, respectively. In fact, this sum (eq 6) which in principle has to be equal to 1, turns out to be equal to 1 ± 0.1 .

3.4. Naphthalene Fluorescence Depolarization.

Figure 6 shows the NP concentration dependence of NP fluorescence anisotropy, r , in a-PS films. At low concentrations of NP less than 1%, r values are averaged to be 0.18. Thus, this value is determined to be the intrinsic anisotropy of NP when each NP molecule is isolated from each other. Even at higher concentrations of NP between 4% and 10%, the r values did not change so much and settled down to be 0.07. Although the decrease from 0.18 to 0.07 appears to be induced by singlet energy migration among NP molecules, this small reduction is quite reasonable because its efficiency is low. Förster mechanism²⁸ is thought to describe

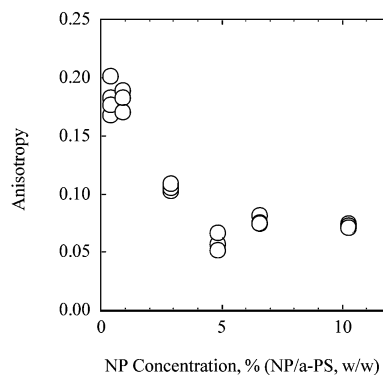


Figure 6. Concentration dependence of NP fluorescence anisotropy, r , in a-PS films prepared by using a spin-coating method. The excitation wavelength is 280 nm. Each point shows the average r value of one film.

Table 2. Fluorescence Anisotropy Values of NP Absorbed into s-PS Films Presenting Different Crystalline Phases

| films | crystallinity degree (%) | thickness (μm) | amount of NP (wt %) | anisotropy |
|--------------|--------------------------|-----------------------------|---------------------|-------------------|
| 1 amorphous | | 60 | <1 | 0.070 ± 0.019 |
| 2 amorphous | | 70 | <1 | 0.064 ± 0.016 |
| 3 α^a | 40 | 20 | 2.5 | 0.071 ± 0.011 |
| | | | | 0.069 ± 0.007 |
| 4 δ | 15 | 70 | 2 | 0.038 ± 0.007 |

^a The α -form semicrystalline film of s-PS was uniaxially stretched. The anisotropy values were measured for orientation of the polarized light plane parallel and perpendicular with respect to the film stretching direction of the α -form film.

singlet energy migration²⁹ and it predicts that even if the distance between them is just 0.735 nm³⁰ the possibility for excitation energy of a NP molecule to migrate to another NP is 50% when they are randomly dispersed.

The fluorescence anisotropy values were measured for NP molecules absorbed in different types of s-PS films and summarized in Table 2. The emission anisotropy value as measured for NP absorbed in amorphous s-PS films is 0.07 and is substantially identical to that measured for NP doped in a-PS films at high concentrations of NP. Taking into account thickness of films and NP concentrations, 0.07 is quite reasonable: the thickness of the a-PS films measured in the present paper is less than 0.5 μm whereas that of the s-PS films is more than 60 μm . Essentially the same anisotropy value has been measured for NP molecules absorbed into α form semicrystalline films (third row of Table 2), where NP molecules can only be absorbed into the amorphous phase.

Definitely smaller r values ($r \approx 0.04$) are instead obtained for NP guest molecules in unoriented s-PS films presenting the NP clathrate phase, where most NP molecules are included in the crystalline phase.

This reduction of fluorescence anisotropy for NP molecules being guest of the s-PS clathrate phase, with respect to those absorbed in polystyrene amorphous phases, could have as usual two alternative interpretations: (i) a larger molecular motion of the chromophore and (ii) a more efficient energy migration among chromophores.

Recent ²H NMR studies on s-PS samples have shown that the mobility of aromatic molecules is larger when they are absorbed in the amorphous phase and lower when they are guest of the nanoporous δ phase.^{31,32} Moreover, the mobility of the large NP guest molecule

is particularly restricted (at least at room temperature), with respect to smaller guests like benzene, toluene or chlorobenzene.³² This is not surprising since its molar volume ($\sim 130 \text{ \AA}^3$) is close to the volume of the cavity ($\sim 120\text{--}160 \text{ \AA}^3$).² As a consequence, higher anisotropy values than for NP molecules absorbed by the amorphous phase would be expected. The observed reduction of anisotropy of fluorescence suggests that microenvironment of NP molecules being guest of the cavities of δ -form crystal, and in particular their distance and orientation, could favor excitation energy transfer.

In this respect, it is worth noting that adjacent guest molecules included in the host crystalline phase present as possible distances $n \times 0.77 \text{ nm}$ (along the c axis), $n \times 0.96 \text{ nm}$ (along the $\langle 101 \rangle$ directions) and $n \times 1.18 \text{ nm}$ (along the b axis), where n is an integer. Moreover, for a given crystallite, all NP guest molecules present essentially the same orientation with respect the crystalline axes of the δ form. This could be the possible reason for a more efficient energy transfer, which could rationalize the observed low values of fluorescence anisotropy.

Conclusions

The achievement of unoriented as well as of axially oriented films of syndiotactic polystyrene presenting the clathrate phase with naphthalene has been shown by X-ray diffraction measurements.

Infrared linear dichroism measurements on axially oriented s-PS films show that NP absorbance peaks are poorly dichroic when NP molecules are simply absorbed in the s-PS amorphous phase while they are highly dichroic when NP molecules are guest of the s-PS clathrate phase. These high dichroic ratios clearly indicate that the NP molecules, when included into the polymeric host lattice present a substantial degree of order with respect to the draw direction.

The order parameter S , as evaluated by the dichroic ratio of NP guest infrared peaks, results to be always positive and negative for out-of-plane and in-plane vibrational modes, respectively. By a quantitative comparison between order parameters of infrared absorption peaks of the helical polymer host and of the NP guest, the α angles between the transition moment vectors and the chain axis of the polymeric host lattice, have been evaluated for guest B_{1u} , B_{2u} , and B_{3u} vibrational modes.

A molecular modeling analysis shows that the energy minimum location of NP into the crystalline cavity (Figure 1B) presents the fused rings plane roughly perpendicular to the chain axis. On the basis of the calculated energy minimum location of NP into the crystalline cavity, the α_{calc} angles between the transition moment vectors and the chain axis of the polymeric host lattice, have been independently calculated.

The comparison between experimentally evaluated and calculated α angles confirms that, for NP guest molecules included into the s-PS/NP clathrate phase, a preferential orientation of the NP fused rings roughly perpendicular to the host chain axis occurs. The comparison also indicated the presence of some limited NP mobility into the clathrate phase (on the time scale of the FTIR measurements) with respect to the average minimum energy position.

As for fluorescence depolarization measurements, it has been shown that NP molecules absorbed into amorphous phases, of a-PS and of amorphous and

semicrystalline (α -form) s-PS films, present the same r values (≈ 0.07). It demonstrates that the microenvironments in amorphous region are the same. Definitely lower r values (≈ 0.04) have been observed for NP molecules being guest of the nanoporous δ -form of s-PS. Since NP guest molecules of the δ form are less mobile than NP molecules adsorbed in the amorphous s-PS phase, the observed reduction of fluorescence anisotropy could be tentatively attributed to a more efficient resonance energy transfer between guest molecules, possibly associated with their ordered positioning and orientation into the host nanoporous polymeric crystallites.

Acknowledgment. Financial support of the "Ministero dell'Istruzione, dell'Università e della Ricerca" (PRIN 2004 and FIRB2001) of "Regione Campania" (Legge 5 and Centro di Competenza per le Attività Produttive) and of a Grant-in-aid for Scientific Research (C) (15550183) from the Ministry of Education, Culture, Sports, Science and Technology of Japan. We thank Dr. Pellegrino Musto of the Institute of Chemistry and Technology of Polymers (CNR) of Naples, Prof. Vincenzo Barone of University of Naples, and Dr. Paola Rizzo and Dr. Alexandra Albulia of the University of Salerno for useful discussions.

References and Notes

- (1) De Rosa, C.; Guerra, G.; Petraccone, V.; Pirozzi, B. *Macromolecules* **1997**, *30*, 4147.
- (2) (a) Milano, G.; Venditto, V.; Guerra, G.; Cavallo, L.; Ciambelli, P.; Sannino, D. *Chem. Mater.* **2001**, *13*, 1506. (b) Tamai, Y.; Fukuda, M. *Polymer* **2003**, *44*, 3279.
- (3) (a) Chatani, Y.; Shimane, Y.; Inagaki, T.; Ijitsu, T.; Yukinari, T.; Shikura, H. *Polymer* **1993**, *34*, 1620. (b) Chatani, Y.; Inagaki, T.; Shimane, Y.; Shikuma, H. *Polymer* **1993**, *34*, 4841.
- (4) De Rosa, C.; Rizzo, P.; Ruiz de Ballesteros, O.; Petraccone, V.; Guerra, G. *Polymer* **1999**, *40*, 2103.
- (5) (a) Guerra, G.; Manfredi, C.; Rapacciuolo, M.; Corradini, P.; Mensitieri, G.; Del Nobile, M. A. Ital. Pat. 1994 (C.N.R.) (b) Reverchon, E.; Guerra, G.; Venditto, V. *J. Appl. Polym. Sci.* **1999**, *74*, 2077.
- (6) (a) Manfredi, C.; Del Nobile, M. A.; Mensitieri, G.; Guerra, G.; Rapacciuolo, M. *J. Polym. Sci., Polym. Phys. Ed.* **1997**, *35*, 133. (b) Musto, P.; Mensitieri, G.; Cotugno, S.; Guerra, G.; Venditto, V. *Macromolecules* **2002**, *35*, 2296. (c) Larobina, D.; Sanguigno, L.; Venditto, V.; Guerra, G.; Mensitieri, G. *Polymer* **2004**, *45*, 429.
- (7) (a) Guerra, G.; Manfredi, C.; Musto, P.; Tavone, S. *Macromolecules* **1998**, *31*, 1329. (b) Musto, P.; Manzari, M.; Guerra, G. *Macromolecules* **1999**, *32*, 2770. (c) Musto, P.; Manzari, M.; Guerra, G. *Macromolecules* **2000**, *33*, 143. (d) Guerra, G.; Milano, G.; Venditto, V.; Musto, P.; De Rosa, C.; Cavallo, L. *Chem. Mater.* **2000**, *12*, 363.
- (8) (a) Sivakumar, M.; Yamamoto, Y.; Amutharani, D.; Tsujita, Y.; Yoshimizu, H.; Takatoshi, K. *J. Appl. Polym. Sci.* **2003**, *89*, 2882. (b) Saitoh, A.; Amutharani, D.; Yamamoto, Y.; Tsujita, Y.; Yoshimizu, H.; Okamoto, S. *Polym. J.* **2003**, *35*, 868. (c) Mohri, S.; Amutharani, D.; Yamamoto, Y.; Tsujita, Y.; Yoshimizu, H. *J. Polym. Sci., B, Polym. Phys.* **2004**, *42*, 238.
- (9) Mensitieri, G.; Venditto, V.; Guerra, G. *Sens. Actuators B* **2003**, *92*, 255.
- (10) Albulia, A. R.; Di Masi, S.; Rizzo, P.; Milano, G.; Musto, P.; Guerra, G. *Macromolecules* **2003**, *36*, 8695.
- (11) Rizzo, P.; Lamberti, M.; Albulia, A.; Ruiz de Ballesteros, O.; Guerra, G. *Macromolecules* **2002**, *35*, 5854.
- (12) (a) Rizzo, P.; Costabile, A.; Guerra, G. *Macromolecules* **2004**, *37*, 3071. (b) Rizzo, P.; Della Guardia, S.; Guerra, G. *Macromolecules* **2004**, *37*, 8043.
- (13) Itagaki, H.; Horie, K.; Mita, I. *Prog. Polym. Sci.* **1990**, *15*, 361.

- (14) Itagaki, H. In *Experimental Methods in Polymer Science: Modern Methods in Polymer Research and Technology*; Tanaka, T., Ed.; Academic Press: New York, 2000; Chapter 3.
- (15) Itagaki, H. *Macromol. Symp.* **2001**, *166*, 13.
- (16) Itagaki, H.; Nakatani, Y. *Macromolecules* **1997**, *30*, 7793.
- (17) (a) Samuels, R. J. In *Structured Polymer Properties*; Wiley: New York, 1971; Chapter 2, pp 28–37. (b) Kakudo, M.; Kasai, N. In *X-ray Diffraction by Polymers*; Elsevier: Amsterdam, 1972; Chapter 10, pp 252–259. (c) Alexander, L. E. In *X-ray Diffraction Methods in Polymer Science*; Krieger, R. E., Ed.; Huntington, NY, 1979; Chapter 4, pp 210–211.
- (18) (a) B. E. Read, In *Structure and Properties of Oriented Polymers*; Ward I. M. Ed.; Appl. Sci. Publishers: London, 1975; Chapter 4, pp 150–184. (b) Jasse, B.; Koenig, J. L. *J. Macromol. Sci.—Rev. Macromol. Chem.* **1979**, *C17*, 61.
- (19) See, e.g.: Califano, S. *Vibrational States*; Wiley: London, 1976; pp 62–65.
- (20) *Gaussian 98*. Frisch, M. J.; Trucks, G. W.; Schlegel, H. B.; Scuseria, G. E.; Robb, M. A.; Cheeseman, J. R.; Zakrzewski, V. G.; Montgomery, J. A., Jr.; Stratmann, R. E.; Burant, J. C.; Dapprich, S.; Millam, J. M.; Daniels, A. D.; Kudin, K. N.; Strain, M. C.; Farkas, O.; Tomasi, J.; Barone, V.; Cossi, M.; Cammi, R.; Mennucci, B.; Pomelli, C.; Adamo, C.; Clifford, S.; Ochterski, J.; Petersson, G. A.; Ayala, P. Y.; Cui, Q.; Morokuma, K.; Malick, D. K.; Rabuck, A. D.; Raghavachari, K.; Foresman, J. B.; Cioslowski, J.; Ortiz, J. V.; Stefanov, B. B.; Liu, G.; Liashenko, A.; Piskorz, P.; Komaromi, I.; Gomperts, R.; Martin, R. L.; Fox, D. J.; Keith, T.; Al-Laham, M. A.; Peng, C. Y.; Nanayakkara, A.; Gonzalez, C.; Challacombe, M.; Gill, P. M. W.; Johnson, B.; Chen, W.; Wong, M. W.; Andres, J. L.; Gonzalez, C.; Head-Gordon, M.; Replogle, E. S.; Pople, J. A. Gaussian, Inc.: Pittsburgh, PA, 1998.
- (21) Reynolds, N. M.; Savage, J. D.; Hsu, S. L. *Macromolecules* **1989**, *22*, 2869.
- (22) Guerra, G.; Musto, P.; Karasz, F. E.; MacKnight, W. J. *Makromol. Chem.* **1990**, *191*, 2111.
- (23) Lippincot, E. R.; O'Reilly, E. J. *J. Chem. Phys.* **1955**, *23*, 238.
- (24) Sellers, H.; Pulay, P.; Boggs, J. E. *J. Am. Chem. Soc.* **1985**, *107*, 6487.
- (25) Martin, J. M. L.; El-Yazal, J.; Francois, J.-P. *J. Phys. Chem.* **1996**, *100*, 15358.
- (26) Reynolds, N. M.; Hsu, S. L. *Macromolecules* **1990**, *23*, 3463.
- (27) Musto, P.; Tavone, S.; Guerra, G.; De Rosa, C. *J. Polym. Sci., Polym. Phys. Ed.* **1997**, *35*, 1055.
- (28) (a) Förster, Th. *Naturwissenschaften* **1946**, *33*, 166. (b) Förster, Th. *Discuss. Faraday Soc.* **1959**, *27*, 7.
- (29) Itagaki, H.; Mita, I. In *Degradation and Stabilization of Polymers*; Jellinek, H. H. G., Ed.; Elsevier: Amsterdam, 1989; Vol. 2, p 45.
- (30) Berlman, I. B. In *Energy Transfer Parameters of Aromatic Compounds*; Academic Press: New York, 1973; p 308.
- (31) Trezza, E.; Grassi, A. *Macromol. Rapid Commun.* **2002**, *23*, 260.
- (32) Albulnia, A. R.; Graf, R.; Guerra, G.; Spiess, H. W. *Macromol. Chem. Phys.*, in press.

MA047863N